JOURNAL OF MATERIALS SCIENCE 28 (1993) 4435–4441

SiO_2–Sm_2O_3 vitreous films via the sol–gel method

M. ZAHARESCU, C. PIRLOG, M. GARTNER
Institute of Physical Chemistry, Splaiul Independentei 202, Bucharest 79611, Romania

F. MOISE
ZECASIN-SA, Splaiul Independentei 202, Bucharest 79611, Romania

V. TEODORESCU
Institute of Physics and Technology of Materials, Bucharest – Magurele, P.O. Box MG-7, Bucharest 76900, Romania

SiO_2–Sm_2O_3 vitreous films 120 nm thick were obtained via the sol–gel method. Infrared, energy-dispersive analysis of X-rays, spectroscopic ellipsometry and absorption spectroscopy showed a total inclusion of samarium in the silica matrix, which remains amorphous up to 1000 °C. The inclusion of the samarium ion increases the porosity. The optical properties of films were investigated by spectro-ellipsometry, and the parameters obtained were compared with those obtained by other techniques.

1. Introduction

The preparation of glass coatings is one of the most important fields of application of the sol–gel technique and many compositions have been produced to enhance some properties or to give new ones to different substrates [1]. An important feature of sol–gel coatings is the ability to control the refractive index through variations of the sol; for example, by pre-aggregating the sol, a porous film with a low index results [2].

Silica films are electrically conducting and infrared-reflecting coatings with a wide range of applications. In the last few years, growing interest has been shown in the production of coloured thin films based on SiO_2 doped with transition metal ions [3–14]. In this paper we present results concerning the preparation and characterization of vitreous SiO_2, containing Sm_2O_3. To our knowledge, vitreous coatings obtained via the sol–gel method for this system have not been reported in the literature.

2. Experimental procedure

The compositions of the initial solutions and the experimental conditions are presented in Table I.

Ethylorthosilicate (Serva) was used as the SiO_2 source, $Sm(NO_3)_3 \cdot H_2O$ (Merck) was the Sm_2O_3 source, and absolute ethylic and methylic alcohol p.a. (Reactivul) were used as solvents and nitric acid p.a. (Reactivul) as the catalyst.

The pH of the initial solution was 6, but in order to maintain the solution viscosity at a low value, the pH was adjusted to 1. The viscosity of the solution before deposition was 1.08 cP.

Thin films were obtained by dip-coating on common glass (silica–soda-lime) previously cleaned. Usually, both faces of the substrate were coated. The withdrawal speed was typically 5 cm min^{-1}.

After each coating procedure, the films were dried and thermally treated to 500 °C, in order to densify them. The solutions and the films obtained from them were characterized as follows. The viscosity of solutions prior to deposition was determined by means of a Höppler viscometer. Differential thermal analysis was carried out using a MOM-OD-103 derivatograph, and infrared spectroscopy was performed on a Carl Zeiss Jena Specord 75 IR Spectrophotometer. X-

TABLE I Solution compositions and experimental conditions

	Sample				
	S_1	S_2	S_3	S_4	S_5
$\frac{C_2H_5OH}{Si(OC_2H_5)_4}$	1.31	1.31	1.31	1.31	1.31
$\frac{CH_3OH}{Si(OC_2H_5)_4}$	11.47	11.47	11.47	11.47	11.47
$\frac{H_2O}{Si(OC_2H_5)_4}$	5.25	5.25	5.25	5.25	5.25
$\frac{Sm(NO_3)_3 \cdot 6H_2O}{Si(OC_2H_5)_4}$	0.1	0.1	0.1	0.1	0.1
pH	1	1	1	1	1
Immersion time (min)	5	5	5	3	1
Temp. of thermal treatment (°C)	500	500	500	500	500
Time of thermal treatment (min)	30	30	30	30	30

0022–2461

ray diffraction measurements were made using a HZG diffractometer, using CuK_α radiation. Energy dispersive X-ray analysis (EDAX) was performed using a Link-System Si–Li detector in the Jeol TEMSCAN 200 CX electron microscopy working at 40 kV.

The determination of the film thickness and the optical and dielectrical constants as a function of wavelength for the SiO_2–Sm_2O_3 film was carried out with a Romanian ellipsometer which allowed a reading accuracy of 1 min for both azimuths. The measurements were performed in air at an angle of incidence $\phi = 70°$.

The absorption spectra in the ultraviolet–visible range were derived from the reflectance spectra with a double-beam spectrophotometer (Specord MHCO, Carl Zeiss, Jena). The slit width used was 1 nm between 190 and 330 nm, and 2 nm between 330 and 900 nm.

The diffuse reflectance spectrum of the powders of SiO_2–Sm_2O_3 and gel was measured against ZnO as a white standard, for an angle of incidence of $\sim 45°$ and an angle of reflection $\sim 0°$.

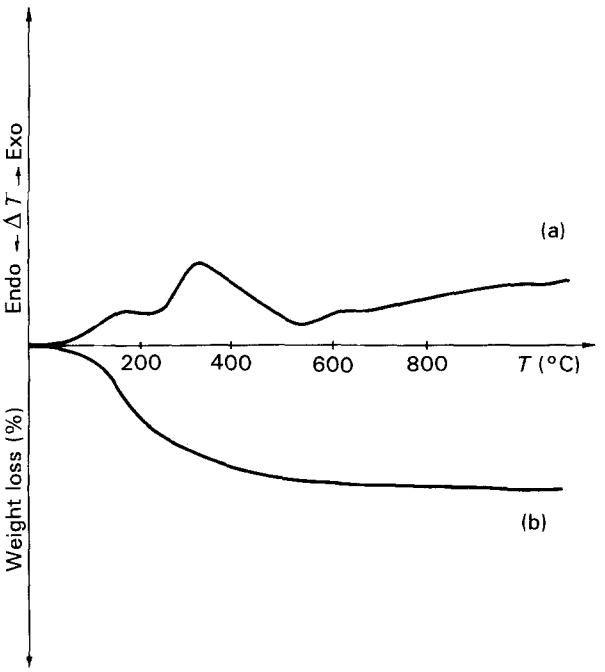

Figure 1 DTA/TGA curves: (a) DTA; (b) TGA.

3. Results and discussion

Continuous, transparent and homogeneous films were obtained using the solution compositions and the experimental conditions given in Table I. A good adherence was obtained for the case of diluted solutions, whose viscosity must not exceed 6 cP. More concentrated solutions with greater viscosity led to defects in the film, such as cracks, and even the possibility of peeling from the substrate. Very good coatings were obtained when the film–substrate bonds were formed before the appearance of strong bonds inside the film [9].

The characteristics of coatings obtained on the SiO_2-Sm_2O_3 system by the above-mentioned methods are discussed and compared below.

3.1. DTA

The thermal treatment of the film densification was performed using the DTA/TGA data. The characterization of the materials obtained after the thermal treatment was carried out both on deposited and unsupported films.

The curves plotted in Fig. 1 show temperatures characteristic for the elimination of water (20–145 °C) and of organic residues (145–485 °C); the total weight loss being 36.25%. Up to 1000 °C, no exotherm effect, i.e. no structural changes of the system, was found. The assignment of the thermal effects recorded by the DTA/TGA were also confirmed by infrared and X-ray analysis.

3.2. Infrared spectroscopy

Fig. 2 show the infrared spectra of the fresh gel (SiO_2-Sm_2O_3), of the gel thermally treated at 500 °C and 1000 °C, respectively, in comparison with those of a pure Sm_2O_3 (Merck). It was found that in the initial

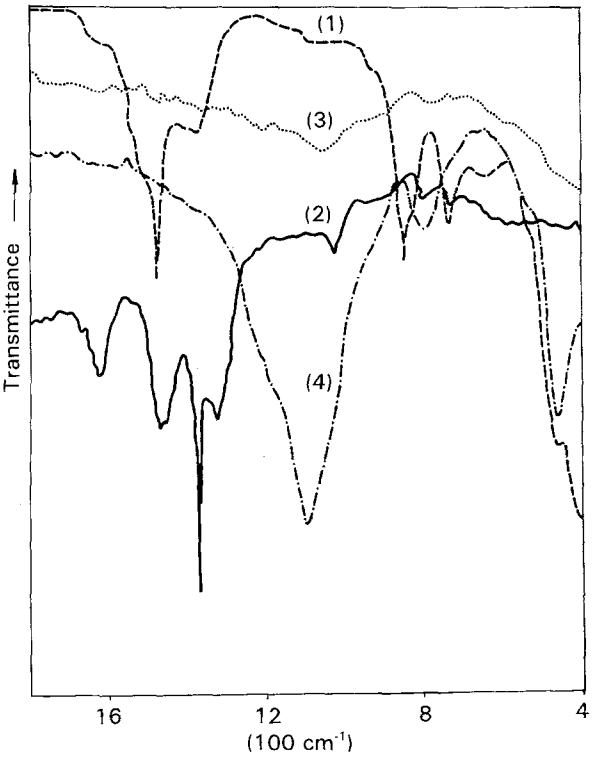

Figure 2 Infrared spectra: (1) pure Sm_2O_3; (2) fresh gel; (3) gel thermally treated at 500 °C; (4) gel thermally treated at 1000 °C.

gel, in addition to the Sm_2O_3 characteristic bands (1475, 1320, 730 cm^{-1} [15]), a band may be observed at 1380 cm^{-1}, attributable to the C–H vibrations in the $-OCH_2CH_3$ [16], and one at 1640 cm^{-1} due to the vibrations of molecular water. After thermal treatment, the shape of the curve was changed. Thus, for the SiO_2–Sm_2O_3 gel thermally treated at 500 °C (Curve 3), the characteristic bands of Sm_2O_3 and those of the organic residues, disappear, and the band characteristic of the SiO_2 glasses obtained via the

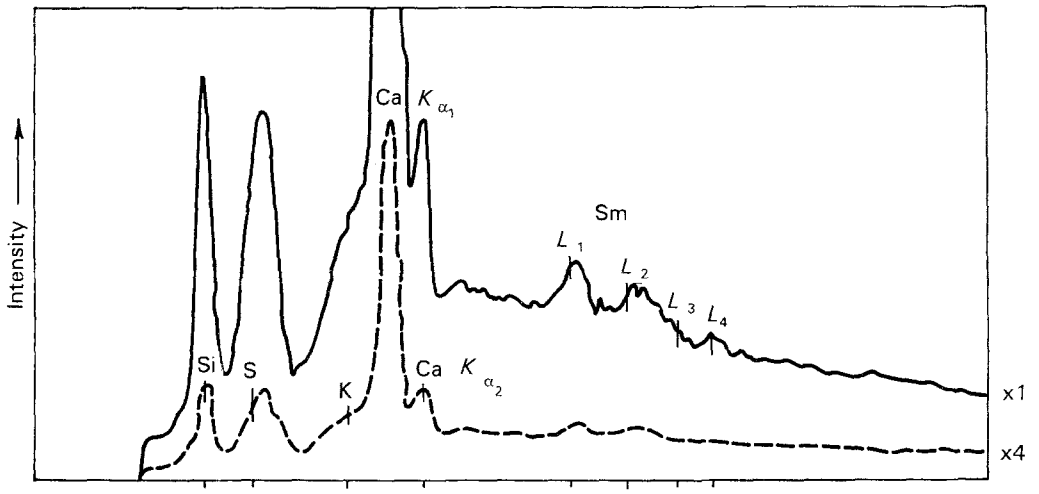

Figure 3 EDAX spectrum for SiO_2–Sm_2O_3 film on glass.

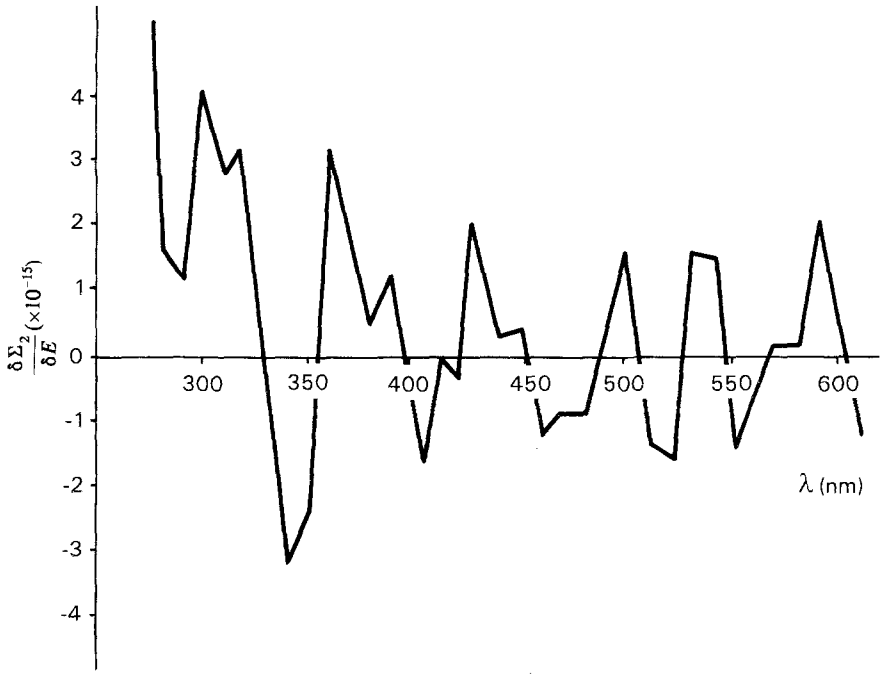

Figure 4 SE spectrum for SiO_2–Sm_2O_3 film on glass.

sol–gel method begins to show up. With increasing temperature, the silicate lattice becomes fixed, and the bands due to the Si–O–Si bonds appear clearly. For the 1000 °C thermally treated gel, the absorption bands can be assigned as follows: 1160–1090 cm^{-1} LO and TO modes of Si–O–Si; 790 and 450 cm^{-1} stretching and bending vibrations of Si–O–Si; the disappearance of Sm_2O_3 bands from the thermally treated gels can be explained by the inclusion of Sm_2O_3 in the SiO_2 matrix.

The degree of the densification and the Si–O band strength increase with increasing of the temperature.

The infrared spectrum characteristic of the vitreous SiO_2 is obtained only after thermal treatment above 1000 °C [17].

3.3. X-ray and EDAX

X-ray diffraction has shown the amorphous character of the SiO_2–Sm_2O_3 film indicating the fact that samarium does not induce crystallization either in the initial stage or after the thermal treatment of the film. The X-ray diffraction results of the film were also confirmed by analysis of the initially unsupported gel thermally treated at 500 and 1000 °C, which retains its amorphous (vitreous) character.

The spectrum obtained by EDAX analysis is presented in Fig. 3. It shows both the elements constituting the support (silica–soda-lime glass) and those of samarium in the SiO_2–Sm_2O_3 film. Further proof of samarium in the SiO_2 matrix is the presence of the four specific L lines.

3.4. Spectro-ellipsometry (SE)

The film thicknesses, calculated from the ellipsometric data, were found to be between 121.4 and 122.5 nm, in agreement with the values in the literature [5]. It is observed that the film thickness does not depend on

the time of immersion of the support in the initial alkoxide.

The optical constants of the SiO_2–Sm_2O_3 film, obtained ellipsometrically in the 270–760 nm range are given in Table II. The inclusion of the samarium in the SiO_2 film leads to a decrease of the refractive index (for $\lambda = 547$ nm, $n_{SiO_2} = 1.457$ and $n_{SiO_2-Sm_2O_3} = 1.350$), i.e. the film becomes more porous. A rough estimate using the equation [18]

$$n_p^2 = (n^2 - 1)(1 - P/100) + 1 \quad (1)$$

where n_p is the refraction index of the porous material, n the refraction index of the non-porous material, and P the porosity, leads to the value $P = 26\%$. This result is particularly important for the preparation of films with the desired porosity by the predetermination of the quantity of lanthanoid ion introduced.

From the experimental data, the complex dielectric functions (ε_1, ε_2) are also calculated (see Table II). The zeros of the derivative of the imaginary part of the dielectric function with respect to the energy (Fig. 4) identify the interband transitions of the SiO_2–Sm_2O_3 film thermally treated at 500 °C, Their values are given in Tables III and IV for the ultraviolet region, and the visible region, respectively. The presence of the Sm^{3+} bands is observed. They can be assigned to the transitions from the level $^6H_{5/2}$ to A, B, C, D, E, F and from $^6H_{7/2}$ to A [15, 19, 20].

The agreement of our data with the literature is good.

TABLE II Optical properties of SiO_2–Sm_2O_3 film determined by ellipsometry; i.e. real and imaginary part of the dielectric function $\langle\varepsilon\rangle$, complex refractive index (n, k)

λ (nm)	ν (cm^{-1})	ε_1	ε_2	n	k
270	37037	1.619	0.547	1.289	0.212
280	35714	1.613	0.311	1.276	0.121
290	34483	1.626	0.404	1.285	0.157
300	33333	1.611	0.244	1.272	0.095
310	32258	1.734	0.128	1.317	0.048
316	31645	1.771	0.084	1.331	0.031
320	31250	1.774	0.040	1.332	0.015
330	30303	1.819	0.004	1.349	0.002
340	29412	1.923	0.051	1.387	0.018
350	28571	1.882	0.172	1.373	0.063
360	27777	1.786	0.175	1.338	0.065
370	27027	1.781	0.029	1.334	0.011
380	26316	1.915	0.074	1.384	0.027
390	25641	2.016	0.018	1.420	0.006
400	25000	2.039	0.015	1.428	0.005
405	24691	2.019	0.025	1.421	0.008
410	24390	1.973	0.045	1.405	0.016
415	24096	1.976	0.028	1.406	0.010
420	23809	1.973	0.046	1.405	0.016
425	23529	1.956	0.034	1.398	0.012
430	23256	1.947	0.011	1.395	0.004
440	22727	1.974	0.036	1.405	0.013
450	22222	1.942	0.005	1.393	0.002
460	21739	1.950	0.022	1.396	0.008
470	21276	1.958	0.041	1.399	0.014
480	20833	1.947	0.046	1.395	0.016
490	20408	1.928	0.064	1.389	0.023
500	20000	1.848	0.031	1.359	0.012
510	19608	1.839	0.021	1.356	0.008
520	19231	1.880	0.064	1.371	0.023
530	18868	1.893	0.057	1.376	0.021
540	18518	1.846	0.030	1.359	0.011
550	18182	1.812	0.024	1.346	0.009
560	17857	1.942	0.058	1.394	0.021
570	17544	1.921	0.040	1.386	0.014
580	17241	1.908	0.054	1.382	0.019
590	16949	1.882	0.038	1.372	0.014
600	16666	1.744	0.014	1.321	0.005
610	16393	1.704	0.016	1.305	0.006
620	16129	1.658	0.037	1.288	0.014
630	15873	1.610	0.024	1.269	0.009
640	15625	1.578	0.016	1.256	0.006
650	15385	1.533	0.030	1.238	0.012
660	15152	1.608	0.050	1.268	0.019
670	14925	1.723	0.042	1.313	0.016
680	14706	1.722	0.056	1.312	0.021
690	14427	1.744	0.017	1.321	0.006
700	14286	1.728	0.016	1.318	0.006
720	13888	1.630	0.074	1.276	0.029
730	13698	1.564	0.039	1.250	0.015
740	13513	1.379	0.097	1.175	0.041
750	13333	1.296	0.113	1.139	0.049
760	13158	1.046	0.108	1.024	0.053

3.5. Absorption spectroscopy

In order to obtain complete data about the SiO_2–Sm_2O_3 system, we also studied the absorption bands of the pure samarium oxide, of the fresh gel and of the gel thermally treated at 500 °C. At these stages the samples are unreflecting, so we could not use the ellipsometry and had to resort to absorption spectroscopy. The results are presented in Tables III and IV, and Fig. 5a and b. From a comparison of the results obtained on the four stages (pure samarium oxide,

TABLE III Absorbtion bands for Sm^{3+} in the ultraviolet range

λ (nm)				
Film	Sm_2O_3	Fresh gel	Thermally treated gel	[19]
	207.3			
			216.0	
		244.0		
	296.0			
	299.0			
		300.0		
			302.0	
			304.0	
	307.3			
	310.6			
			315.3	
	319.0			
329.2				
	334.0			
		344.0	344.0	
	348.0			
		352.0	352.0	
354.3	354.0	354.0		
		356.0		
			360.0	
		362.0		362.0
	366.0		366.0	
		368.0		
	370.0			374.6
				390.2
		392.0		
		394.0		
396.8				

TABLE IV Absorption bands for Sm^{3+} in the visible range

λ (nm)						
Film	Sm_2O_3	Fresh gel	Thermally treated gel	[19]	[20]	[20] Trans.
		402.0	402.0	402.0		
	408.0					
		412.0				
			414.0			
	416.0	416.0	416.0	415.0		
				416.0		
	420.0			418.0	418.4	$^6H_{5/2} \rightarrow F$
420.8						
			428.0			
	432.0	432.0				
			438.0			
		440.0				
				443.0		
	444.0					
				451.0		
452.5			452.0		452.3	$^6H_{5/2} \rightarrow E$
	456.0	456.0				
		464.0		464.0		
	468.0					
		470.0				
	474.0		474.0			
		478.0				
	480.0			472–487		
485.8						
				489.2		
					491.4	$^6H_{5/2} \rightarrow D$
		496.0				
			498.0			
	500.0	500.0	500.0	499.5	500.0	$^6H_{5/2} \rightarrow C$
	504.0					
505.4						
			516.0			
	518.0					
524.9						
			526.0			
					529.1	$^6H_{5/2} \rightarrow B$
	532.0					
			538.0			
			540.0			
		542.0	542.0			
545.1						
		546.0				
	560.0	560.0				
			562.0		561.8	$^6H_{5/2} \rightarrow A$
	564.0					
	566.0					
568.0						
	578.0	578.0	578.0			
	580.0	580.0	580.0			
			582.0			
					595.3	$^6H_{7/2} \rightarrow A$
				599.0		
604.7						

fresh gel, gel thermally treated at 500 °C, SiO_2–Sm_2O_3 film) the following conclusions were drawn.

(a) In the ultraviolet range (Fig. 5a), the main difference between the fresh gel and the gel thermally treated at 500 °C consists in the practically total vanishing of the broad band (270–340 nm) following thermal treatment. The thermally treated gel instead displays two very poorly contoured bands at 304 and 315 nm.

TABLE V Shifts of the absorption bands of samarium in different surroundings

Sm [13, 14]		Sm_2O_3		Film			Fresh gel			Thermally treated gel				
ν_1 (cm^{-1})	λ_1 (nm)	ν_2 (cm^{-1})	$\nu_1 - \nu_2$ (cm^{-1})	ν_3 (cm^{-1})	$\nu_1 - \nu_3$ (cm^{-1})	$\nu_2 - \nu_3$ (cm^{-1})	ν_4 (cm^{-1})	$\nu_1 - \nu_4$ (cm^{-1})	$\nu_2 - \nu_4$ (cm^{-1})	ν_5 (cm^{-1})	$\nu_1 - \nu_5$ (cm^{-1})	$\nu_2 - \nu_5$ (cm^{-1})
23 920	418	23 810	+ 110	23 760	+ 160	+ 50	24 010	− 90	− 200	24 010	− 90	− 200
22 570	443	22 520	+ 50	–	–	–	22 730	− 160	− 210	22 830	− 260	− 310
22 170	451	21 930	+ 240	22 100	+ 70	− 170	21 930	+ 240	0	22 130	+ 40	− 200
21 550	464	21 370	+ 180	–	–	–	21 550	0	− 180	–	–	–
20 830	480	20 830	0	20 590	+ 240	+ 240	20 920	− 90	− 90	21 100	− 270	− 270
20 000	500	20 000	0	19 790	+ 210	+ 210	20 000	0	0	20 000	0	0
18 900	529	18 800	+ 100	19 050	− 150	− 250	–	–	–	–	–	–
–	–	18 450	–	18 345	–	+ 105	Scarcely observable bands					
17 830	562	17 670	+ 130	17 605	+ 225	+ 65	17 860	− 30	− 190	17 800	+ 30	− 130
16 690	599	16 540	+ 50	16 540	+ 150	0	Scarcely observable bands					

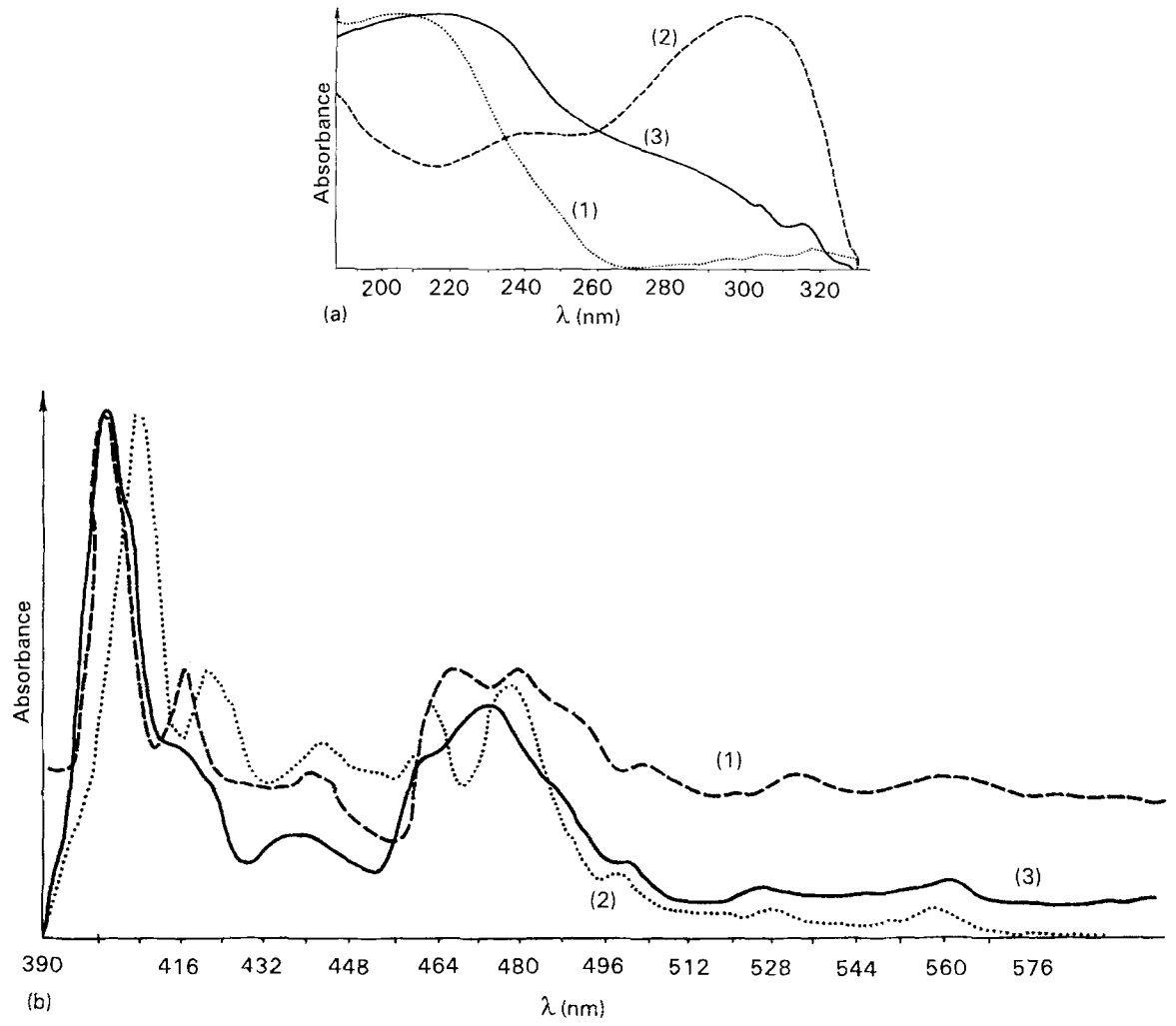

Figure 5 Absorption spectra of (1) Sm_2O_3, (2) fresh gel, (3) thermally treated gel, (a) in the ultraviolet range, (b) in the visible range.

(b) In the visible range, we observe (Fig. 5b) that the absorption bands of the film are subject to a bathochrome shift (Table V) both with respect to the bands of the Sm^{3+} ion in solution [19, 20] and with respect to the bands appearing in pure Sm_2O_3.

(c) The fact that in Sm_2O_3 the same bands are observed as for the Sm^{3+} ion in solution (the shifts due to the change of the hydrated ion Sm^{3+} into the oxide are very small, up to several hundreds of cm^{-1}) shows that in the oxide the chemical bonds between the metallic ion and the oxygen atoms have a partially ionic character. (In the opposite case of a strong covalency, these bands would have been shifted, up to the complete disappearance of the bands of the hydrated lanthanoid ion from the oxide spectrum.)

(d) At the change from the fresh gel to the thermally treated gel, a more or less important shift is observed only for the bands of 418, 443 and 451 nm (shifts greater than 200 cm^{-1}) assigned to the transitions as in Table IV.

(e) In the pure Sm_2O_3 spectrum, the number of intense bands is greater than that of the fresh gel spectrum, and even greater than that of the gel thermally treated at 500 °C (Fig. 5b). The absorption maxima become more and more attenuated as Sm_2O_3 is included in the SiO_2 matrix.

4. Conclusions

Homogeneous and stable films for the SiO_2–Sm_2O_3 system have been obtained using the sol–gel method.

The inclusion of samarium in the SiO_2 matrix is total (as shown by all the experimental methods used: IR, XRD, EDAX, SE and absorption spectroscopy in the ultraviolet–visible range), leading to the disordering of the SiO_2 lattice, and contributing to the preservation of the vitreous character of the material, even for temperatures higher than 1000 °C. At the same time, the inclusion of the ion lowers the refractive index, i.e. gives rise to an increased porosity. This may lead to a wide range of applications.

References

1. S. SAKKA, K. KAMIYA, K. MAKITA and Y. YAMAMOTO, *J. Non-Cryst. Solids* **63** (1984) 223.
2. A. J. HURD and C. J. BINKER, *J. Phys. France* **49** (1988) 1017.
3. A. DURAN, J. M. FERNANDEZ NAVARRO, P. CASARIEGO and A. JOGLER, *J. Non-Cryst. Solids* **82** (1986) 391.
4. K. ARAI, H. NAMIKAWA, K. KUMATO, T. HONDA, Y. ISHII and T. HANDO, *J. Appl. Phys.* **59** (1986) 3430.
5. N. D. S. MOHALLEM and M. A. AEGERTER, *J. Non-Cryst. Solids* **100** (1988) 526.
6. M. A. SAINZ, A. DURAN and J. M. FERNANDEZ NAVARRO, *ibid.* **121** (1989) 315.

7. A. TSUZUKI, H. MURAKAMI, K. KANI, S. KAWAKAMI and Y. TORI, *J. Mater. Sci. Lett.* **9** (1990) 624.
8. M. ZAHARESCU, C. PIRLOG, M. CRISAN, M. GARTNER, M. SAHINI and A. VASILESCU, *Rev. Roum. Chim.* **37** (1992) 173.
9. S. SAKKA, *Bull. Inst. Chem. Res. Kyoto Univ.* **61** (1983) 376.
10. J. STRAWBRIGE and P. F. JAMES, *J. Non-Cryst. Solids* **82** (1986) 366.
11. F. ORGAZ and R. RAWSON, *ibid.* **82** (1986) 376.
12. S. SAKKA and S. ITO, *ibid.* **71** (1985) 311.
13. A. DURAN, P. MAZON, A. JOGLAR and J. M. F. NAVARRO, *Rev. della Staz. Sper. Vetro.* **6** (1986) 59.
14. A. DURAN, J. M. FERNANDEZ NAVARRO, P. MAZON and A. JOGLER, *J. Non-Cryst. Solids* **100** (1988) 494.
15. S. HYAMA and P. SINHA, "Complexes of the Rare Earths" (Pergamon Press, London, 1966) p. 109.
16. H. YOSHINO, K. KAMIYA and H. NASU, *J. Non-Cryst. Solids* **126** (1990) 68.
17. M. ZAHARESCU, C. PIRLOG, M. CRISAN, M. SAHINI, A. BRAILEANU and N. DRAGAN, *Rev. Roum. Chim.* **35** (1990) 589.
18. B. E. YOLDAS, *Appl. Opt.* **19** (1980) 1425.
19. H. REMY, "Lehrbuch der Anorganischen Chemie" (Akademische Verlagsgesellschaft Geest und Portig K.G., Leipzig, 1961) p. 577.
20. LANDOLT-BORNSTEIN, "Atom und Molekularphysik", Vol. 4 (Springer-Verlag, Berlin, Gottingen, 1955) p. 897.

Received 18 March 1992
and accepted 3 February 1993